peak on Jan 30 and then decreased on January 31. This trend was similar to that for $NO_2$ and $SO_2$. Different trends are considered to be related to the different formation mechanisms of aerosols. Based on the different trends exhibited by species during different periods, we classified the pollution process into three stages. Stage 1 was from January 24 to January 26, in which inorganic ions, pollutant gasses, and $PM_{2.5}$ followed the same decreasing trends; stage 2 was from January 26 to the noon of January 30, in which inorganic ions followed $PM_{2.5}$, but pollutant gasses did not vary substantially; and stage 3 was from January 30 to January 31, in which inorganic ions followed the decreasing trend of pollutant gasses, while $PM_{2.5}$ maintained an increasing trend.

### 3.2.1 Stage 1 (January 24 to January 26)

During this period, the concentration of $PM_{2.5,}$ AQI, $SO_2$, $NO_2$, and $SO_4^{2-}$, $NO_3^-$ and $NH_4^+$ decreased. $PM_{2.5}$, AQI, $SO_4^{2-}$, $NO_3^-$ and $NH_4^+$ exhibited the lowest value (69 μg $m^{-3}$, 50.14 μg $m^{-3}$, 14.1μg $m^{-3}$, and 8.0 μg $m^{-3}$) on January 26.

The formation of sulfate is complicated, and it was divided into homogeneous process and heterogeneous reaction. For homogeneous process, it included gas phase reactions of $SO_2$ and free radical (OH, etc), and $SO_2$ dissolved in the water to form $H_2SO_3$ and then oxidized by the oxidant ($H_2O_2$ ect) to sulfate. For heterogeneous processes, it included $SO_2$ react with OH, $O_3$ or $H_2O_2$ to produce sulfate which occurred in the aqueous surface layer preexisting particle. So the

homogeneous process maybe show that the sulfate corrected well with SO2. And the heterogeneous reaction will be the main factor if the sulfate is a function of RH (Liang J.Y and Jacobson M.Z.A, 1999). That means the heterogeneous conversion rates from SO2 to sulfate was sensitive to huminity (McMurry and Wilson, 1983). Fig. 5 demonstrates that sulfate poorly corrected with $SO_2$ ($R^2$ = 0.373) and the sulfate concentrations decreased with the RH, which suggests that the reduction in sulfate levels in Stage 1 might be from heterogeneous processes. Fig. 6 displays the wind speed at this stage, which suggests the air velocity was not strong. Therefore, the wind direction may have caused the pollutants to rapidly disperse and the haze to clear. The details are provided in Section 3.4.

Just like the sulfate, nitrate also can form from $NO_2$ through homogeneous reactions between $HNO_3$ and $NH_3$ or heterogeneous reaction of nitrogen species ($HNO_3$, $NO_3$, and $N_2O_5$ ect). The gas-to-particle partitioning of $NH_4NO_3$ is mainly ruled by RH and temperature. Fig. 5 showed the nitrate corrected well with $NO_2$ ($R^2$ = 0.638), suggesting that the nitrate concentration was mainly affected by $NO_2$, and the nitrate might form through homogeneous reactions of $NO_2$ with $O_3$ or OH to form $HNO_3$ in the gas phase during daytime, while through heterogeneous during the night due to the meteorology condition, which then reacts with $NH_3$ to form $NH_4NO_3$ through the gas-to-particle partition (Wang. et al., 2007). This assumption also supports the relationship between nitration and humidity, and the nitrates increased with the humidity.

### 3.2.2 Stage 2 (January 26 to the noon of January 30)

From January 26 to 10:00 AM January 29, the concentration of $PM_{2.5}$, $NO_2$, $SO_2$, $SO_4^{2-}$, $NO_3^-$, and $NH_4^+$ did not significantly increase. Fig. 7 displays the 4-hour averaged time variations of $PM_{2.5}$ mass concentration, ion concentration, $SO_2$ and $NO_2$ concentrations, and meteorological conditions during the entire measurement period. The ion concentration (sulfate, nitrate, and ammonium) sharply increased, and they increased by 1.86-, 1.66- and 1.39-fold on average, changing from 19.77, 32.16, and 20.73 μg $m^{-3}$ to 56.54 , 85.62, and 49.54 μg $m^{-3}$, respectively, from 10:00 AM on January 29 to 10:00 AM on January 30 during Stage 2. In this stage, the PM2.5 mass changed marginally from 132.7 μg $m^{-3}$ to 144.3 μg $m^{-3}$. During this time, the RH was only approximately 40%–60%, and the temperature was approximately 30–50°F. Therefore, the hygroscopic growth of particles was not the main reason for the increased particle levels in Stage 2. Moreover, the concentrations of ions were higher than those in two massive firework burning events (Section 3.2.3); thus, fireworks were also not the main reason.

The sulfur oxidation ratio (SOR, SOR = n-$SO_4^{2-}$ / (n-$SO_4^{2-}$ + n-$SO_2$).) and the nitrogen oxidation ratio (NOR, NOR = n-$NO_3^-$ / (n- $NO_3^-$ + n- $NO_2$).) are the main parameters. They can be used as indications of the secondary formation.

According to Seinfeld (1986), the gas–phase oxidation of $SO_2$ to $SO_4^{2-}$ by an OH radical is a strong function of temperature. Fig. 8 indicates that the SOR was corrected with $SO_4^{2-}$ ($R^2$ = 0.45), suggesting the formation of sulfate in Stage 2 could not be mainly from gas–phase oxidation and the heterogeneous process. Thus, sulfur oxidation might be not the main process. Therefore, transportation may be the other

reason for the increasing trend.

A pronounced increase in the concentration of nitrate was observed. Moreover, daily cycles were found for this concentration, with peak concentration in the morning, followed by decreases in the afternoon, which is similar to the trend for sulfate. This is because the nitrate concentration is driven by HNO3 production related to gas-to-particle partitioning to form ammonium nitrate, which is more prevalent at lower temperature and higher relative humility. However, the $NO_2$ concentration increased slowly, and the nitrate concentration reached a sharp peak, indicating that regional transportation may have a critical role in controlling nitrate concentrations (Zhang. et al., 2005). Fig. 8 reveals that the NOR corrected well with nitrate ($R^2$ = 0.91), which suggests that nitrate was formed through homogeneous reactions of $NO_2$ with O3 or OH to form $HNO_3$ in the gas phase, which then reacts with $NH_3$ to form $NH_4NO_3$(Wang. et al., 2007). The NOR levels were higher than SOR levels, which was in agreement with the formation rate of nitrate being approximately ten times higher than that of sulfate ( Hewitt C.N, 2001).

Ammonium showed a trend similar to that for sulfate and nitrate, which indicates that it presents mainly in the form of ammonium sulfate and ammonium nitrate.

### 3.2.3 Stage 3 (from the afternoon of January 30 to January 31)

In the measurement period, Chinese New Year occurred on January 31. A different trend was found for pollution on January 30 and January 31. On Chinese New Year's Eve, two massive firework burning events almost occur in the evening (at

approximately 5:00 PM–8:00 PM, for the family reunion dinner), and at midnight (around 00:00 AM–3:00 AM, to celebrate the New Year). Fig. 7 reveals that the firework event had an obvious effect on fine particle concentrations. $PM_{2.5}$ exhibited its maximum concentration for those two episodes, which was 258 μg $m^{-3}$ at 8:00 PM on January 30 and 263 μg $m^{-3}$ at 3:00 AM on January 31. The average concentration of $PM_{2.5}$ increased 0.8-fold, changing from approximately 140 μg $m^{-3}$ to 260 μg $m^{-3}$. The concentrations of sulfate, nitrate, and ammonium were high from 6:00 PM on January 30 to 6:00 AM on January 31. The concentrations of sulfate, nitrate, and ammonium were 37.62 μg $m^{-3}$, 56.63 μg $m^{-3}$, and 34.63 μg $m^{-3}$ at 6:00 PM on January 30, they were 32.14 μg $m^{-3}$, 31.14μg $m^{-3}$, and 26.35 μg $m^{-3}$ at 2:00 AM on January 31, and they were 48.86 μg $m^{-3}$, 25.49 μg $m^{-3}$, and 32.09 μg $m^{-3}$ at 6:00 AM on January 31, respectively.

Fig. 7 suggests that the $PM_{2.5}$ mass fraction was very high, but the ion (sulfate, nitrate, and ammonium) mass fractions were lower during the firework events. Therefore, one reason is possible that the mass fractions of the carbon compounds、Cl and K were very high, and the other reason maybe be the hygroscopic growth of particles during this period. The RH was approximately 66% at 5:00 PM, and it increased to 90% at 8:00 PM (it began to rain), and this level lasted until 6:00 AM on January 31. The concentrations of sulfate, nitrate, and ammonium began to decrease during this measurement period and may have been a result of aerosol wet scavenging (Sun. et al., 2011). Zhang et al. (2015) also revealed that the burning of fireworks emits a large fraction of aerosol particles in the size range of 1–2.5 μm, and volatile

organic compounds (VOCs) play a role in the aerosol phase during firework displays. Wang et al. (2007) showed the ions (sulfate、nitrate、ammonium) would increase in the firework times. However, compared with that in Stage 2, the concentrations of ions in the two massive firework burning events were lower, which means that aerosol wet scavenging had a greater effect on ions than did fireworks during this period. While the hygroscopic growth of particles maybe affect the concentration of PM2.5 during this period.

The fireworks could (Wang et al. 2007, Zhang et al. 2015) could be one factor for the pollution during the firework events. But in our paper, aerosol wet scavenging and the hygroscopic growth of particles had a great effect on pollution.

## 3.3 Cation and anion balance

To determine the reasons for the formation of pollution in different stages, we also studied the cation and anion balance in PM2.5.

The calculations of the equivalence of cations and anions are obtained through the following equations:

$$\text{Cation equivalence} = NH_4^+/18.04 \quad (1)$$

$$\text{Anion equivalence} = NO_3^-/62.005+2*SO_4^{2-}/96.06 \quad (2)$$

Fig. 9 reveals a high correlation between the calculated equivalence of cations and anions, with $R^2 > 0.94$. This finding indicates that $NH_4^+$ exists in the air with ammonium sulfate and ammonium nitrate, and the slope indicates that the air was neutralized during the measurement period in Zhengzhou.

During the measurement period (January 24 to January 31), the nitrate to sulfate ratios were approximately 1–2, which indicated that nitrate was more likely to be formed than sulfate. This phenomenon is similar to that observed in particle studies in Taiwan and Beijing. The most abundant anions of PM2.5 were $Cl^-$, nitrate (5.49 Ave), and sulfate (2.03 Ave). Tsai, et al. (2012) discovered that the mass fraction of nitrate was higher than sulfate during Taiwan's Lantern Festival, and Jiang et al. (2015) reported that nitrate levels increased faster than sulfate levels during a firework display in Beijing.

The mass ratio of nitrate to sulfate has been employed as an indicator of the relative importance of stationary versus mobile sources of sulfur and nitrogen in the atmosphere (Arimotoet al., 1996; Yao et al., 2002; Wang et al., 2006). In China, the ratios are different in cities in different seasons. Lai (2007) suggested reported a ratio of 0.36–0.68 in PM2.5 at eight sites in winter. Fig. 10 displays the time series of the mass ratio of nitrate to sulfate. In this study, nitrate to sulfate ratios were in the range of 0.52–1.72, with a mean of 1.29. These ratios were much higher than that in Beijing (0.71) and Shanghai (0.64) (Wang. et al., 2005). Excluding the firework period (10:00 PM on January 30 to 6:00 PM on January 31), nitrate to sulfate ratios were in the range of 0.77–1.72, with a mean of 1.33, which were still higher than that in Beijing. During the heavy firework period, the ratios decreased rapidly from approximately 1.6 to 0.6, which is similar to that reported by Tian et al. (2014), who revealed that the mass ratios of nitrate to sulfate during the heavy firework period were lower than those during the light firework period. This

suggests that although stationary sources, such as power plants and other industrial sources of emission, are crucial contributors, mobile sources of emissions should not be neglected in winter in Zhengzhou.

## 3.4 Source of pollution

For Stage 1, Fig. 11 reveals that the wind from the east of Zhengzhou was clear air, which resulted in the rapid dispersal of pollutants and the clearing of haze. Duo (2016) studies the transportation of Zhengzhou and also revealed the wind from the east could decrease the concentration of the pollution.

For Stage 2, transport was one of the main sources of pollution, in particular from 10:00 PM (14:00PM, UTC) on January 29 to 2:00 PM (6:00AM, UTC) on January 30, when the concentrations of sulfate, nitrate, ammonium, $SO_2$, and $NO_2$ increased rapidly. To study the regional transport of PM2.5 from neighboring sources, air mass trajectories were downloaded from the website (https://ready.arl.noaa.gov/hypub-bin/trajtype.pl) to study the sources of pollution. During the measurement period, the air mass trajectories revealed that air mass at 500 m was mainly from the northwest, and the pollutant concentration increased. The air mass originated from the northwest and traveled across Shanxi Province and Shaanxi Province, and might contain a large amount of pollutants from the northwestern polluted areas. Consequently, pollutant concentrations may have increased. Huang et al. (2017) also revealed that $PM_{2.5}$ concentrations in Shijiazhuang, which originated from Inner Mongolia and passed over Shanxi Province to arrive at the sampling

location, resulted in the highest $PM_{2.5}$ value (178.9 μg $m^{-3}$). Fig. 6 showed the ground wind speed was about 5-7 km/h which came from the northwest from 10:00 PM on January 29 to 2:00 AM on January 30. The pollutions would increased. And then the wind speed began to decreased to 0-4km/h which made the pollutions began to assemble. The wind increased to about 7-9 km/h, the region transport from 10:00AM on January 30 to 2:00 PM (6:00AM, UTC) on January 30.

For Stage 3, Pollution particles dispersed only after 6:00 PM (10:00AM, UTC) on January 30, when the wind direction changed from northwest to south and the wind speed decreased. Subsequently, Chinese New Year followed, and the fireworks display occurred, resulting in increased emissions of sulfur compounds and nitrogenous compounds. However, from Fig. 11, the effect of transportation from the northwest was greater than the local source of pollution.

Therefore, in Zhengzhou, the pollution from east clears and the pollution from the northwest increases which was similar with the result of Hebei (Huang et al. 2017). The pollutions would be easy to assemble in the stable meteorological conditions.

## 4. CONCLUSION

Inorganic compounds in $PM_{2.5}$ were measured using FTIR from January 24 to January 31, 2014, in Zhengzhou. By combining the data of gases ($NO_2$ and $SO_2$), particle mass concentration ($PM_{2.5}$), and meteorological parameters, the daily variation and time series of pollution were analyzed. According to the trend of

pollution, the measurement period was divided into three stages. Pollution levels were low during Stage 1 (January 24 to January 26). The nitrate corrected well with $NO_2$ ($R^2$ = 0.89), suggesting that the nitrate concentration was mainly affected by $NO_2$, and the sulfate corrected well with humidity ($R^2$ = 0.72), but poorly corrected with $SO_2$ (0.054), suggesting that the formation of sulfate in Stage 1 may have mainly been a result of the heterogeneous process. The wind from the east of Zhengzhou was one main reason why pollutants were rapidly dispersed and the haze cleared. In Stage 2 (January 26 to noon on January 30), the SOR corrected poorly with $SO_4^{2-}$ ($R^2$ = 0.45), indicating that transportation was the main reason for the high sulfate concentration. In this stage, NOR corrected well with nitrate ($R^2$ = 0.91), suggesting that nitrate was formed through the homogeneous gas–phase reactions of $NO_2$ with OH or $O_3$ to form $HNO_3$ in $PM_{2.5}$. In Stage 3 (afternoon of January 30 to January 31), the average concentration of $PM_{2.5}$ changed from approximately 140 μg $m^{-3}$ to 260 μg $m^{-3}$, and the concentrations of sulfate, nitrate, and ammonium changed from 37.62, 56.63, and 34.63 μg $m^{-3}$ to 32.14, 31.14, and 26.35 μg $m^{-3}$, respectively. The hygroscopic growth of particles may be the primary reason for the high $PM_{2.5}$ levels in this period. the cation (Ammonium) corrected well with the anions (sulfate and nitrate) ($R^2$ = 0.94). This finding indicates that $NH_4^+$ exists in air with ammonium sulfate and ammonium nitrate, and the slope indicates that the air was neutralized during measurement period in Zhengzhou. The nitrate to sulfate ratios were approximately 1–2. This finding suggests that although stationary sources, such as

power plants and other sources of industrial emissions, are critical contributors, mobile sources of air pollution should not be neglected in winter in Zhengzhou. It (nitrate to sulfate ratio) was low during the heavy firework period. A backward trajectory cleared the pollution from the east and increased the pollution from the northwest in Zhengzhou.

## ACKNOWLEDGMENTS

This work was supported by the National Natural Science Foundation of China (No. 91544218 and No. 41375027) and The Science and Technological Fund of Anhui Province for Outstanding Youth (No.1808085J19). We thank the Department of Environmental Protection of Henan Province for use of their location for sampling.

## Reference

Arimoto, R., Duce, R. A., Savoie, D. L. Prospero, J. M., Talbot, R., Cullen, J. D., Tomza, U.,Lewis, N. F., Ray, B. J. (1996). Relationships among aerosol constituents from Asia and the North Pacific during PEM-West A. *J Geophys Res.* 101(D1): 2011–2023.

Chan, C.K. and Yao, X. (2008). Air pollution in mega cities in China. *Atmos. Environ.* 42(1): 1-42.

Chang, Y. H., Deng, C., Cao, F., Cao, C., Zou, Z., Liu, S. D., Lee, X. H., Li, J., Zhang, G., and Zhang，Y. L. (2017). Assessment of carbonaceous aerosols in Shanghai, China: Long-term evolution, seasonal variations and meteorological effects，*Atmos. Chem. Phys.*, 17: 9945-9964

Duo, K.Z., (2016). Formation mechanism and control strategies of atmospheric haze:Specialized research results of atmospheric haze in Henan province,

496 China Environmental Science Press, Beijing.( in Chinese)

497 Lai, S. C, Zou S. C., Cao J. J., Lee S. C., Ho, K. F. (2007). Characterizing ionic species in
498 PM2.5 and PM10 in four Pearl River Delta cities, South China, *J. Environ. Sci.* 19:939–
499 947

500 Coury, C., Dillner, A. M. (2008). A method to quantify organic functional groups and
501 inorganic compounds in ambient aerosols using attenuated total reflectance FTIR
502 spectroscopy and multivariate chemometric techniques. *Atmos. Environ.* 42: 5923– 5932.

503 Feng, J. L., Yu, H., Su, X. F., Liu, S. H., Li, Y., Pan, Y. P., Sun, J. H. (2016). Chemical
504 composition and source apportionment of PM2.5 during Chinese Spring Festival at
505 Xinxiang, a heavily polluted city in North，China: Fireworks and health risks, *Atmos. Res*.
506 182:176–188.

507 Godri, K. J., Green, D. C., Fuller, G. W., OSTO, M. D., Beddows, D. C., Kelly, F. J.,
508 Harrison, R. M., and Mudway, I. S.(2010) .Particulate oxidative burden associated with
509 firework activity, *Environ. Sci. Technol*. 44: 8295–8301.

510 Hewitt, C.N., (2001). The atmospheric chemistry of sulfur and nitrogen in power station
511 plumes. *Atmos. Environ*. 35: 1155–1170.

512 Huang, X. J., Liu, Z. R., Liu, J. Y., Hu, B., Wen, T. X., Tang, G. Q., Zhang, J. K., Wu, F. K.,
513 Ji, D. S., Wang, L. L., Wang, Y. S., (2017). Chemical characterization and synergetic
514 source apportionment of PM2.5 at multiple sites in the Beijing-Tianjin-Hebei region,
515 China, *Atmos. Chem. Phys. (Discussion)*. 231: 871-881.

516 Jiang, Q., Sun, Y. L., Wang, Z. F., Yin, Y. (2015). Aerosol composition and sources during
517 the Chinese Spring Festival: fireworks, secondary aerosol, and holiday effects, *Atmos.*
518 *Chem. Phys.* 15: 6023–6034.

519 Kadir, M.F.Z., Aspanut, Z., Majid, S.R., Arof, A.K. (2011). FTIR studies of plasticized
520 poly(vinyl alcohol)–chitosan blend doped with NH4NO3 polymer electrolyte membrane.
521 *Spectrochimica Acta Part A.* 78:1068–1074.

522 Kong, S. F., Li, L., Li, X. X., Yin, Y., Chen, K., Liu, D. T., Yuan, L., Zhang, Y. J., Shan, Y.
523 P., and Ji, Y. Q. (2015).The impacts of firework burning at the Chinese Spring Festival
524 on air quality: insights of tracers, source evolution and aging processes, *Atmos. Chem.*
525 *Phys*.15:2167-2184.

526 Lai, S. C., Zou, S. C., Cao, J. J., Lee, S. C., Ho, K. F., (2007). Characterizing ionic species in
527 PM2.5 and PM10 in four Pearl River Delta cities, South China. *Journal of*
528 *Environmental Sciences.* 19: 939 – 947.

529 Li, H. Y., Zhang, Q., Zhang, Q., Chen, C. R., Wang, L. T., Wei, Z., Zhou, S., Parworth, C.,
530 Zheng, B., Canonaco, F., Prevot, A. S. H., Chen, P., Zhang, H. L., Wallington, T. J., He，
531 K. B. (2017). Wintertime aerosol chemistry and haze evolution in an extremely polluted
532 city of the North China Plain: significant contribution from coal and biomass combustion.
533 *Atmos. Chem. Phys.* 17: 4751-4768

534 Liang. J.Y., Jacobson, M.Z. (1999). A study of sulfur dioxide oxidation pathways over a
535 range of liquid water contents, PHs and temperature. *Advances in Air Pollution 6 (Air*
536 *pollution VII)*. P989-996.

537 Liao, X.N., Zhang, X.L., Wang, Y.C., Liu, W.D., Du, J. and Zhao, L.H. (2014). Comparative
538 analysis on meteorological condition for persistent haze cases in summer and winter in
539 Beijing. *J. Environ. Sci.-China.* 35: 2031-2044

540 Liu, J. H., Zhang, Y. H., Wang, L. Y., Wei, Z. F. (2005). Drawing out the structural
541 information of the first layer of hydrated ions: ATR-FTIR spectroscopic studies on
542 aqueous NH4NO3, NaNO3, and Mg(NO3)2 solutions. *Spectrochimica Acta Part A.*
543 6:1893–899

544 Liu, N., Wei, X. L., Gao, M. G., Xu, L. (2015). A Quantitative Analysis Method of
545 Water-Soluble Inorganic Ions with ATR-FTIR Spectroscopy. Spectroscopy and
546 Spectral Analysis (in chinese). 35(12):3364-3368

547 McMurry, P. H., Wilson, J. C. (1983). Droplet phase (Heterogeneous) and gas phase
548 (homogeneous) contributions to secondary ambient aerosol formation as functions of
549 relative humidity. *J Geophys Res, C: Oceans and Atmospheres.* 88:5101-5108.

550 Jiang, N., Guo, Y., Wang, Q., Kang, P. R., Zhang R. Q., Tang, X. Y. (2017). Chemical
551 Composition Characteristics of PM2.5 in Three Cities in Henan, Central China. *Aerosol*
552 *and Air Quality Research*.17: 2367–2380

553 Pope, C. A., Dockery, D. W. (2006). Health effects of fine particulate air pollution: Lines that
554 connect. *J. Air Waste Manage Assoc*. 56:709-742.

555 Reff, A., Turpin, B. J., Porcja, R. J., Giovenntti, R., Cui, W., Weisel, C. P., Zhang. J., Kwon,
556 J., Alimokhtari, S., Morandi, M., Stock, T., Maberti, S., Colome, S., Winer, A., Shendell,
557 d., Jones, J., Farrar, C., (2005). Functional group characterization of indoor, outdoor, and
558 personal $PM_{2.5}$ results from RIOPA. *Indoor Air.* 15: 53-61.

559 Seinfeld, J.H., 1986. Atmospheric Chemistry and Physics of Air Pollution. Wiley, New York,
560 P348.

561 Shang, X. N., Lee, M., Meng, F., Wang, S. H., Suh, I., Kim, D., Jeon, K., Wang, X. Z., Zhao,
562 Y. X., Zhang，K., (2017). Characteristics and source apportionment of fine haze aerosol
563 in Beijing during the winter of 2013. *Atmos. Chem. Phys. (Discussion),* 515.

564 Steven, F. M., Lynn M. R., Barbara J. T., Robert J. P., (2002). FTIR measurements of
565 functional groups and organic mass in aerosol samples over the Caribbean. *Atmos.*
566 *Environ*. 36: 5185–5196.

567 Sun, Y. L., Jiang, Q., Wang, Z. F., Fu, P. Q., Li, J., Yang, T., Yin, Y., (2014). Investigation of
568 the sources and evolution processes of severe haze pollution in Beijing in January 2013.
569 *J. Geophys. Res. Atmos.* 119: 4380-4398.

570 Sun, Y. L., Zhang, Q., Schwab, J. J.， Chen, W. N., Bae, M. S., Lin, Y. C., Hung, H. M.,
571 Demerjian, K. L., (2011). A case study of aerosol processing and evolution in summer in
572 New York City, *Atmos. Chem. Phys.*, 11:25751-25784.

573 Tai, A. P. K., Mickley, L. J., Jacob, D. J., Leibensperger, E. M., Zhang, L., Fisher, J. A.,
574 Pye, H. O. T. (2012). Meteorological modes of variability for fine particulate matter
575 (PM2.5) air quality in the United States: implications for PM2.5 sensitivity to climate
576 change. *Atmos. Chem. Phys*. 12: 3131-3145

577 Tao, J., Zhang, L. M., Cao, J. J., Zhang, R. J. (2017). A review of current knowledge
578 concerning PM2.5 chemical composition, aerosol optical properties, and their
579 relationships across China. *Atmos. Chem. Phys.* 17:9485-9518

580 Tian, M., Wang, H. B., Chen, Y., Yang, F. M., Zhang, X. H., Zou, Q., Zhang, R. Q., Ma, Y.
581 L., He, K. B. (2016). Characteristics of aerosol pollution during heavy haze events in
582 Suzhou, China. *Atmos. Chem. Phys.* 16:7357–7371.

583 Tian, Y. Z., Wang, J., Peng, X., Shi, G. L., Feng, Y. C. (2014). Estimation of the direct and
584 indirect impacts of fireworks on the physicochemical characteristics of atmospheric
585 PM10 and PM2.5, *Atmos. Chem. Phys*. 14:9469–9479.

586 Tsai, H. H., Chien, L. H., Yuan, C. S., Lin, Y. C., Jen, Y. H., and Ie, I. R.(2012). Influences of
587 fireworks on chemical characteristics of atmospheric fine and coarse particles during
588 Taiwan's Lantern Festival. *Atmos. Environ.* 62: 256–264.

589 Tsai, Y. I., Kuo, S. C., (2006). Development of diffuse reflectance infrared Fourier transform
590 spectroscopy for the rapid characterization of aerosols. *Atmos. Environ.* 40:1781–1793.

591 Wang, J., Wang, S., Jiang, J., Ding, A., Zheng, M., Zhao, B., Wong, D.C., Zhou, W., Zheng,
592 G., Wang, L., Pleim, J.E. and Hao, J. (2014b). Impact of aerosol–meteorology
593 interactions on fine particle pollution during China's severe haze episode in January
594 2013. *Environ. Res. Lett*. 9: 094002.

595 Wang, J., Li, X., Zhang, W., Jiang, N., Zhang, R. and Tang, X. (2015). Secondary PM2.5 in
596 Zhengzhou, China: Chemical species based on three years of observations. Aerosol Air
597 Qual. Res. 16: 91–104

598 Wang, S., Yu, S. C., Li, P. F., Wang, L. Q., K., Liu, W. P., Yan , R. C., Zheng, X. J., (2017).
599 A Study of Characteristics and Origins of Haze Pollution in Zhengzhou, China, Based on
600 Observations and Hybrid Receptor Models. *Aerosol and Air Quality Research.* 17: 513–
601 528.

602 Wang, Y., Zhuang, G. S., Xu, C., Zheng, A. H., (2007). The air pollution caused by the
603 burning of fireworks during the lantern festival in Beijing, *Atmos. Environ.* 41:417-431.

604 Wang, Y., Zhuang, G. S., Tang, A. H., Yuan, H., Sun, L. L., Chen, S., Zheng, A. H., (2005).
605 The ion chemistry and source of PM2.5 aerosol in Beijing. *Atmos. Environ.* 39: 3771–
606 3784.

607 Wang, Y., Zhuang, G. S., Zhang, X. Y., Huang, K., Xu, C., Tang, A. H., Chen, J. M., An, Z.
608 S., (2006). The ion chemsitry, seasonal cycle, and sources of PM2.5 and TSP aerosol in
609 Shanghai. *Atmos. Environ.*40: 2935–2952.

610 Xiao, Z.M., Zhang, Y.F., Hong, S.M., Bi, X.H., Jiao, L., Feng, Y.C. and Wang, Y.Q. (2011).
611 518 Estimation of the main factors influencing haze, based on a long-term monitoring
612 campaign 519 in Hangzhou, China. *Aerosol Air Qual. Res.* 11: 873—882.

613 Yao, X. H., Chan, C. K., Fang, M., Cadle, S., Chan, T., Mulawa, P., He, K. B., Ye, K. B.,
614 (2002). The water-soluble ionic composition of PM2.5 in Shanghai and Beijing, China.
615 *Atmos. Environ.* 36: 4223–4234.

616 Zhang, J. S., Chen, Z. Y., Lu, Y.H., Gui, H.Q., Liu, J. G., Liu, W. Q., Wang, J., Yu, T. Z.,
617 Cheng, Y., Chen, Y., Ge, B. Z., Fan, Y., Luo, X. S. (2017). Characteristics of aerosol
618 size distribution and vertical backscattering coefficient profile during 2014 APEC in
619 Beijing, *Atmos. Environ.*148: 30-41

620 Zhang, R., Wang, G., Guo, S., Zamora, M. L., Ying, Q., Lin, Y., Wang, W., Hu, M., and
621 Wang, Y.(2015). Formation of urban fine particulate matter, *Chem. Rev.* 115:
622 3803-3855.

623 Zhang, Q., Canagaratna, M. R., Jayne, J. T., Worsnop, D. R., Jimenez, J. L. (2005). Time- and
624 size-resolved chemical composition of submicron particles in Pittsburgh: Implications
625 for aerosol sources and processes. *J. Geo. Res.* 110: D07S09.

626
627
628
629
630
631
632
633

**Table 1.** ATR—absorption frequencies and vibrational modes of observed

**Table 2.** The air quality in Zhengzhou during the measurement period.

678
679
680
681
682
683
684
685
686
687
688
689
690
691
692
693
694
695
696
697
698
699
700
701
702
703
704
705
706
707 **Table 1.** ATR—absorption frequencies and vibrational modes of observed species
708 on PM2.5.

| Wavenumber($cm^{-1}$) | Species | Vibration mode |
|---|---|---|
| 825 | Nitrate, | $\nu_2$ |
| 1044 | Sulfate | $n_{asym}$ (SO4)- $n_3$ |
| 1074 | Sulfate | $n_{asym}$ (SO4)- $n_3$ |
| 1182 | Hydrogen sulfate | $C_{3v}$ |
| 1321 | Nitrate | $\nu 3$ |
| 1412 | Ammonium | $NH_4^+$ deformation |
| 3033 | Ammonium | $\nu_2+\nu_4$ |
| 3186 | Ammonium | $\nu_3$ |

709
710
711
712

**Table 2.** Air quality in Zhengzhou during the measurement period.

| Date | AQI | $PM_{2.5}$( μg $m^{-3}$) | Air quality level(CMEP) |
|---|---|---|---|
| 2014/1/24 | 245 | 195 | Heavily Polluted |
| 2014/1/25 | 179 | 135 | Moderately Polluted |
| 2014/1/26 | 69 | 50 | Good |
| 2014/1/27 | 115 | 87 | Lightly Polluted |
| 2014/1/28 | 133 | 101 | Lightly Polluted |
| 2014/1/29 | 182 | 137 | Moderately Polluted |
| 2014/1/30 | 243 | 193 | Heavily Polluted |
| 2014/1/31 | 314 | 209 | Severely Polluted |

**Fig.1.** The location of the collection site.

**Fig.2.** FTIR–ATR spectra of PM2.5.

**Fig.3.** The daily variability of the PM2.5, SO2, NO2 concentration and AQI.

**Fig.4.** (a) The daily variability of the PM2.5、sulfate、nitrate and ammonium. （b）The daily variability of temperature and humility.

**Fig.5.** Scatterplot and linear regression analysis of (a) $NO_3^-$ and $NO_2$;(b) $SO_4^{2-}$and $SO_2$.

**Fig.5(b).** Time series of wind speed.

**Fig.6.** Time series of meteorologic parameters and pollutant concentration measured during measurement period.

**Fig.7.** Scatterplot and linear regression analysis of (a)$NO_3^-$ and NOR; (b) $SO_4^{2-}$and SOR.

**Fig. 8.** (a) Time series of cation, anion and the acidity in PM2.5 (b) The correction between cation and anion (c) Time series of wind speed.

**Fig.9** time series of the mass ratio of nitrate/sulfate

**Fig.10** Backward trajectory determined by the National Oceanic and Atmospheric Administration Hybrid Single Particle Lagrangian Integrated Trajectory (HYSPLIT) model



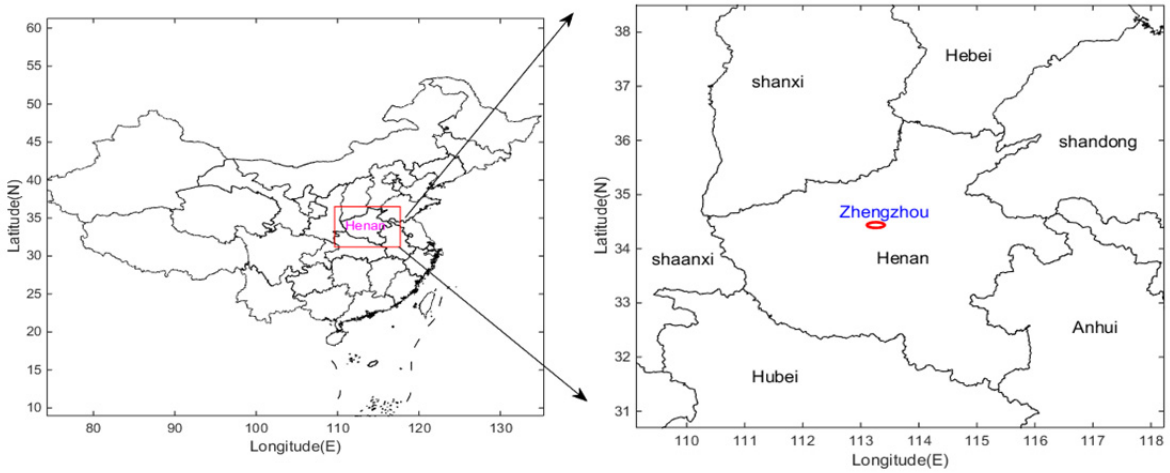


**Fig.1.** Location of the collection site.

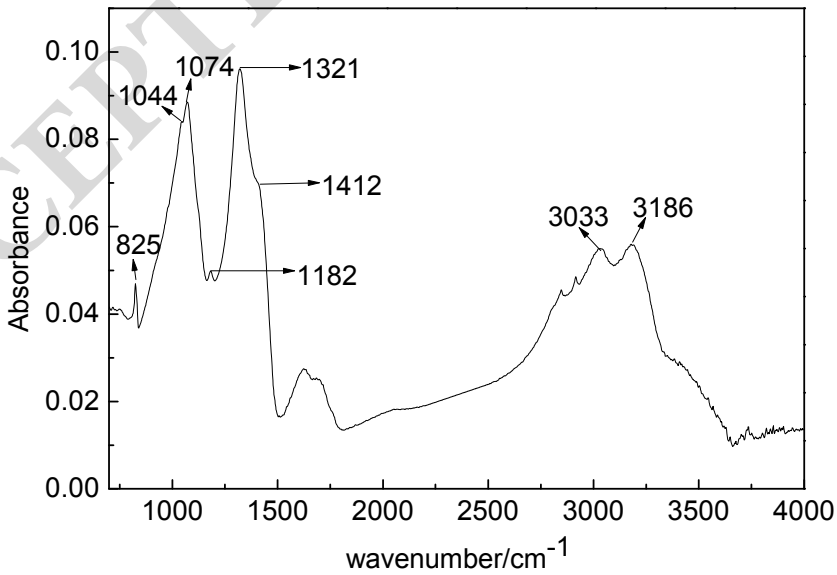


**Fig.2.** FTIR–ATR spectra of PM2.5.

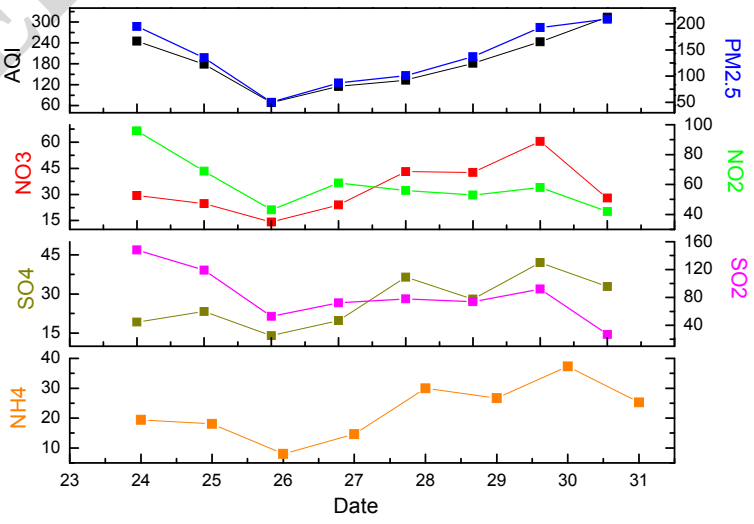

**Fig.3.** Daily variability of $PM_{2.5}$, $NO_2$, $SO_2$, $NO_3^-$, $SO_4^{2-}$, $NH_4^+$ concentrations and AQI.

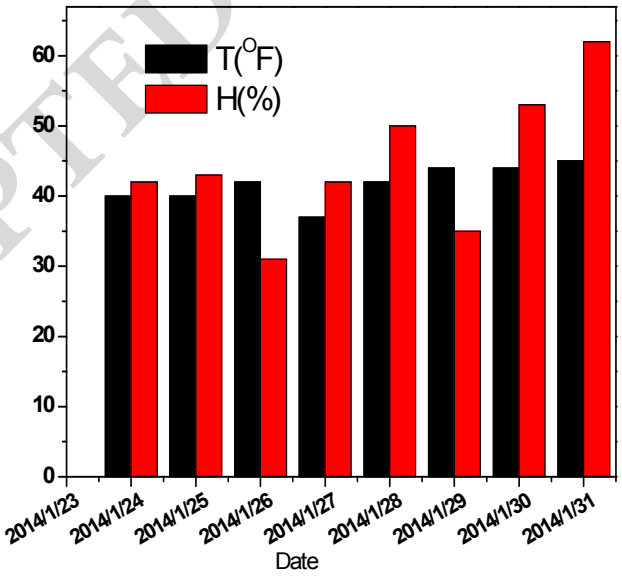


**Fig.4.** Daily variability of temperature and humidity.

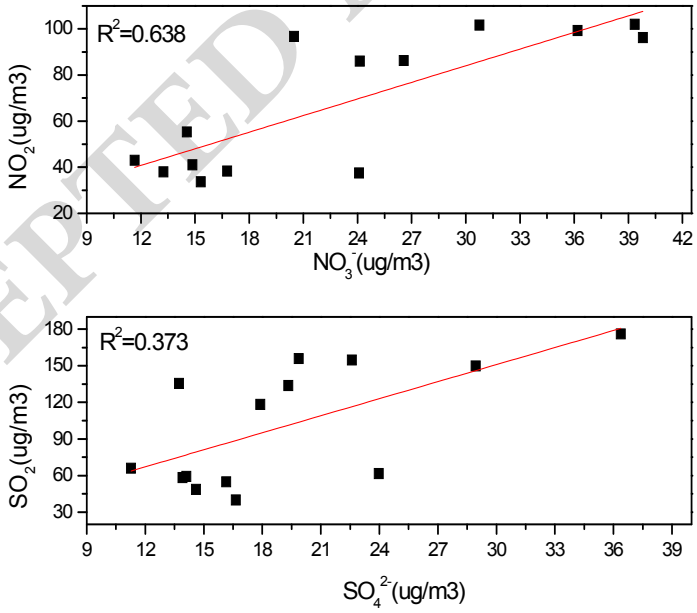


**Fig. 5** Scatter plot and linear regression analysis of $NO_3^-$ and $NO_2$; $SO_4^{2-}$ and $SO_2$.

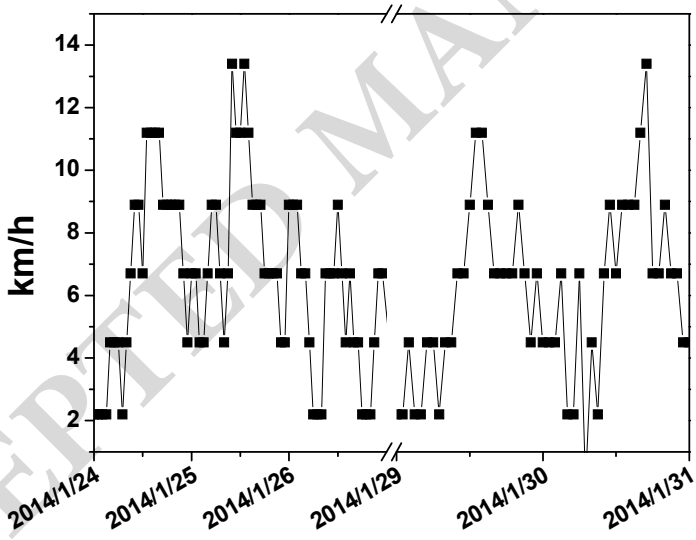


**Fig. 6** Time series of wind speed.

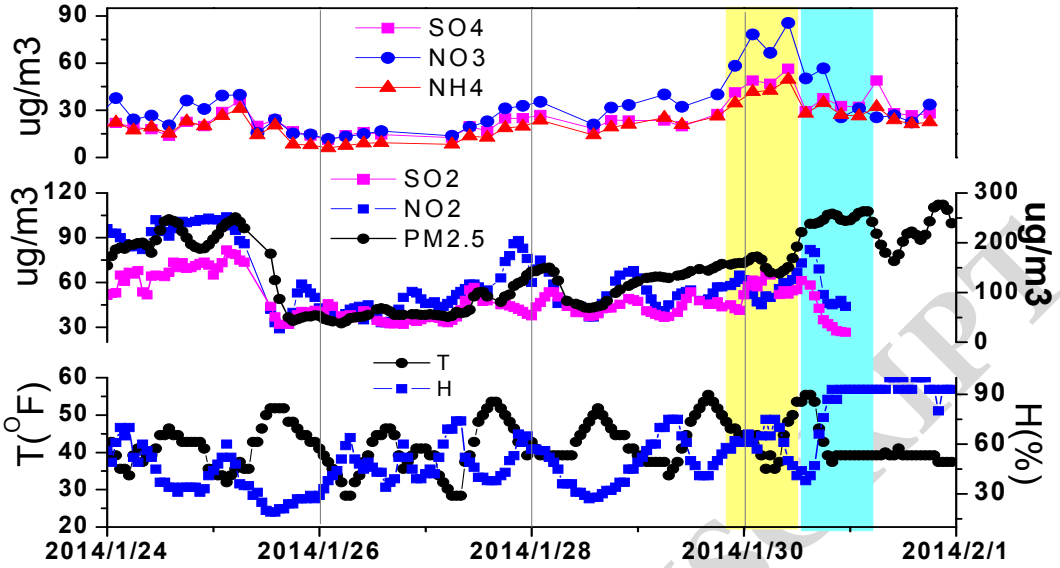


**Fig.7.** Time series of meteorologic parameters and pollutant concentration measured during the measurement period.

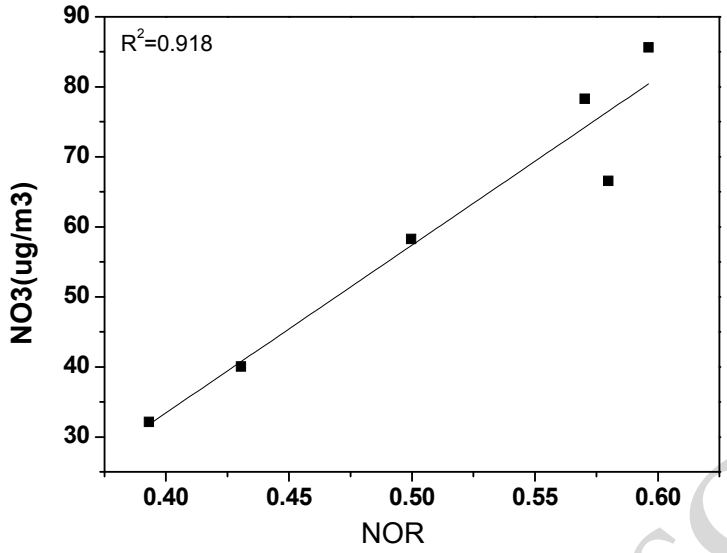


(a)

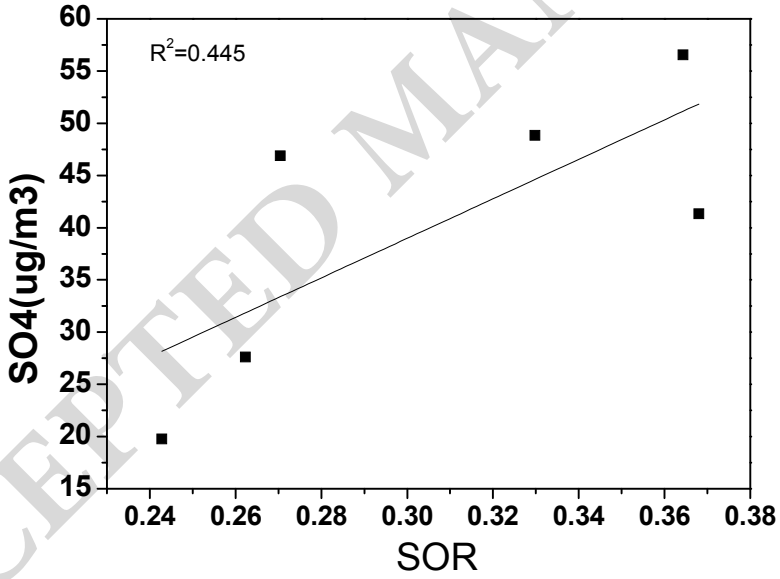


(b)

**Fig 8.** Scatterplot and linear regression analysis of (a) $NO_3^-$ and NOR; (b) $SO_4^{2-}$ and SOR.

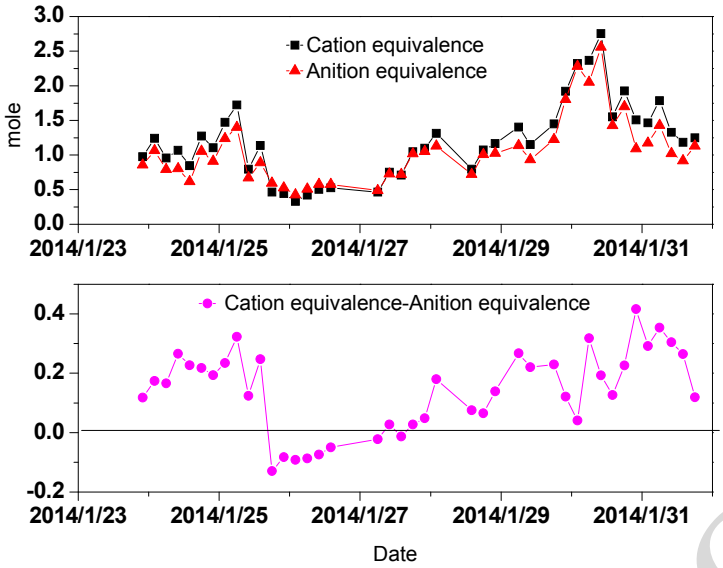


(a)

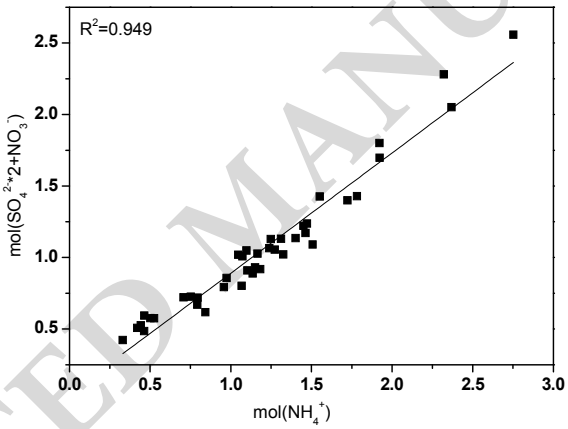


(b)

**Fig. 9.** (a) Time series of cation and anion levels and the acidity in PM2.5 (b) Correlation between cation and anions

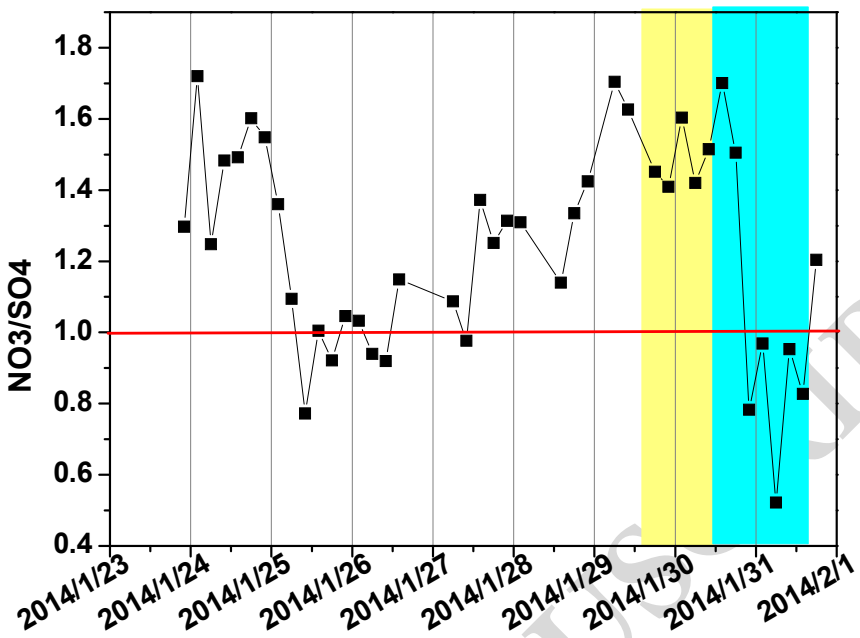


**Fig.10** Time series of the mass ratio of nitrate/sulfate

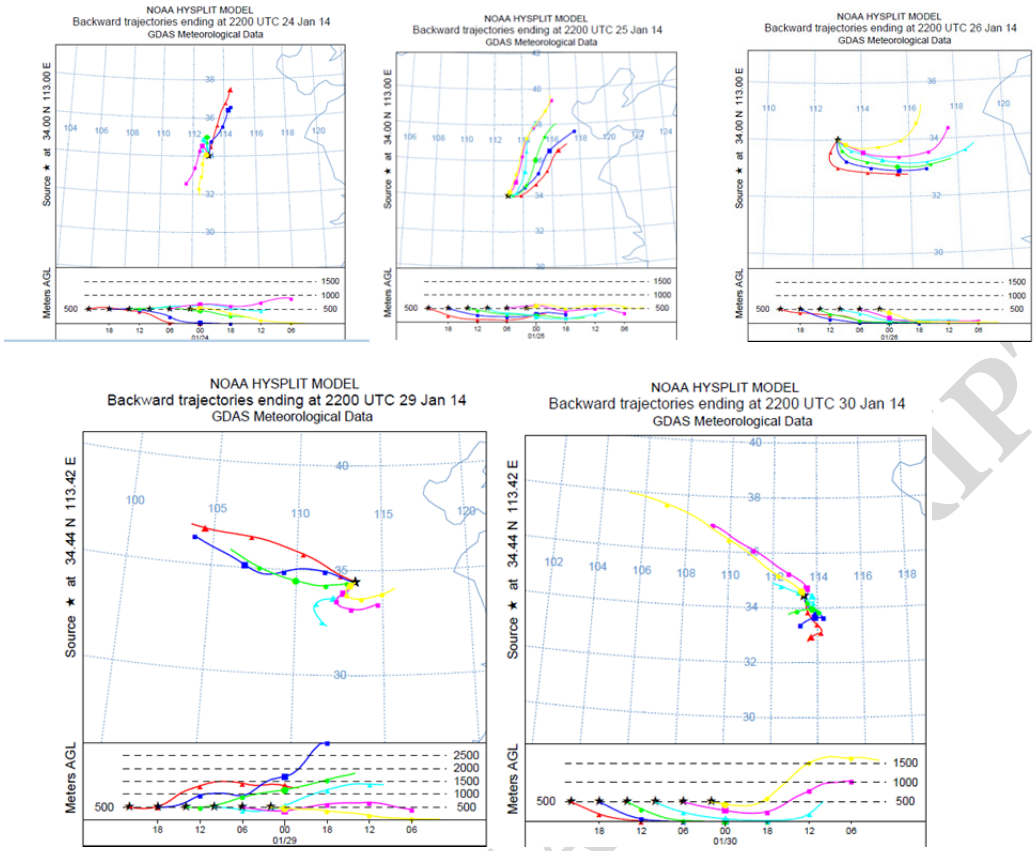


**Fig.11** Backward trajectory determined by the National Oceanic and Atmospheric Administration Hybrid Single Particle Lagrangian Integrated Trajectory (HYSPLIT) model